KLHL12 can form large COPII structures in the absence of CUL3 neddylation

Tamara Moretti[a,†], Kyungho Kim[b,†], Astha Tuladhar[a], and Jinoh Kim[a,*]
[a]Department of Biomedical Sciences, College of Veterinary Medicine, Iowa State University, Ames, IA 50011;
[b]Targeted Therapy Branch, National Cancer Center, Goyang, Gyeonggi 10408, Republic of Korea

ABSTRACT **CUL3-RING ubiquitin ligases (CRL3s) are involved in various cellular processes through different Bric-a-brac, Tramtrack, and Broad-complex (BTB)–domain proteins. KLHL12, a BTB-domain protein, is suggested to play an essential role in the export of large cargo molecules such as procollagen from the endoplasmic reticulum (ER). CRL3^{KLHL12} monoubiquitylates SEC31, leading to an increase in COPII vesicle dimension. Enlarged COPII vesicles can accommodate procollagen molecules. Thus, CRL3^{KLHL12} is essential for the assembly of large COPII structures and collagen secretion. CRL3s are activated by CUL3 neddylation. Here, we evaluated the importance of CUL3 neddylation in COPII assembly and collagen secretion. Unexpectedly, the assembly of large COPII-KLHL12 structures persisted and cellular collagen levels decreased on treatment with MLN4924, a potent inhibitor of NEDD8-activating enzyme. When we introduced mutations into KLHL12 at the CUL3 interface, these KLHL12 variants did not interact with neddylated CUL3, but one of them (Mut A) still supported large COPII–KLHL12 structures. Overexpression of wild-type KLHL12, but not Mut A, lowered cellular collagen levels most likely via lysosomal degradation. Our results suggest that CUL3 neddylation is not necessary for the formation of large COPII–KLHL12 structures, but active CRL3^{KLHL12} contributes to the maintenance of collagen levels in the cell.**

Monitoring Editor
Elizabeth Miller
MRC Laboratory of Molecular Biology

Received: Aug 31, 2022
Revised: Jan 3, 2023
Accepted: Jan 9, 2023

INTRODUCTION

CUL3-RING ubiquitin (Ub) ligases (CRL3s) are the major E3 ligase family in eukaryotes (Petroski and Deshaies, 2005a). They usually associate with a RING-IBR-RING ligase (RBR)-type E3 ligase, ARIH1, to ubiquitylate target substrates (Scott *et al.*, 2016). A CRL is composed of a catalytic module and a substrate recognition module (Petroski and Deshaies, 2005a). In CRL3s, a Bric-a-brac, Tramtrack, and Broad-Complex (BTB) domain protein serves as the substrate recognition module (Furukawa *et al.*, 2003; Pintard *et al.*, 2003; Xu *et al.*, 2003). BTB domain proteins such as KCTD5 and SPOP can mediate mono- and polyubiquitylation of diverse substrates (He *et al.*, 2018; Wang *et al.*, 2020). There are 183 genes with a BTB domain in the human genome (Stogios *et al.*, 2005), indicating that CUL3 is involved in various cellular processes through these BTB-domain proteins. Recent studies have shown that CRL3s are important regulators of different cellular and developmental processes such as mitosis, cytokinesis, cell death, gene expression control, Hedgehog signaling, and WNT signaling, where different BTB-domain proteins are involved (see Genschik *et al.* [2013] for review). Defects of CRL3s have been implicated in metabolic diseases, dystrophies, and cancers (Genschik *et al.*, 2013).

KLHL12 is a BTB-domain protein and CRL3^{KLHL12} is suggested to play an essential role in procollagen export from the ER by ubiquitylating SEC31, a component of a COPII coat (Jin *et al.*, 2012; McGourty *et al.*, 2016). The COPII coat consisting of SAR1, SEC23/SEC24 complex, and SEC13/SEC31 complex is able to generate transport vesicles at the ER exit sites that can package most soluble

This article was published online ahead of print in MBoC in Press (http://www.molbiolcell.org/cgi/doi/10.1091/mbc.E22-08-0383) on January 18, 2023.

†These authors contributed equally to this work.

Author contributions: T.M., K.K., and J.K. designed the study; T.M., K.K., and A.T. collected the data; T.M., K.K., and J.K. wrote the article; and all contributed to editing and reviewing the submission.

*Address correspondence to: Jinoh Kim (jinohk@iastate.edu).

Abbreviations used: BTB, Bric-a-brac, Tramtrack, and Broad-complex; CRL, CUL3-RING ubiquitin ligase; ECM, extracellular matrix; ER, endoplasmic reticulum; FBS, fetal bovine serum; HSF, human skin fibroblast; ned, neddylated; RNAi, RNA interference; siRNA, small interfering RNAs; Ub, ubiquitin.

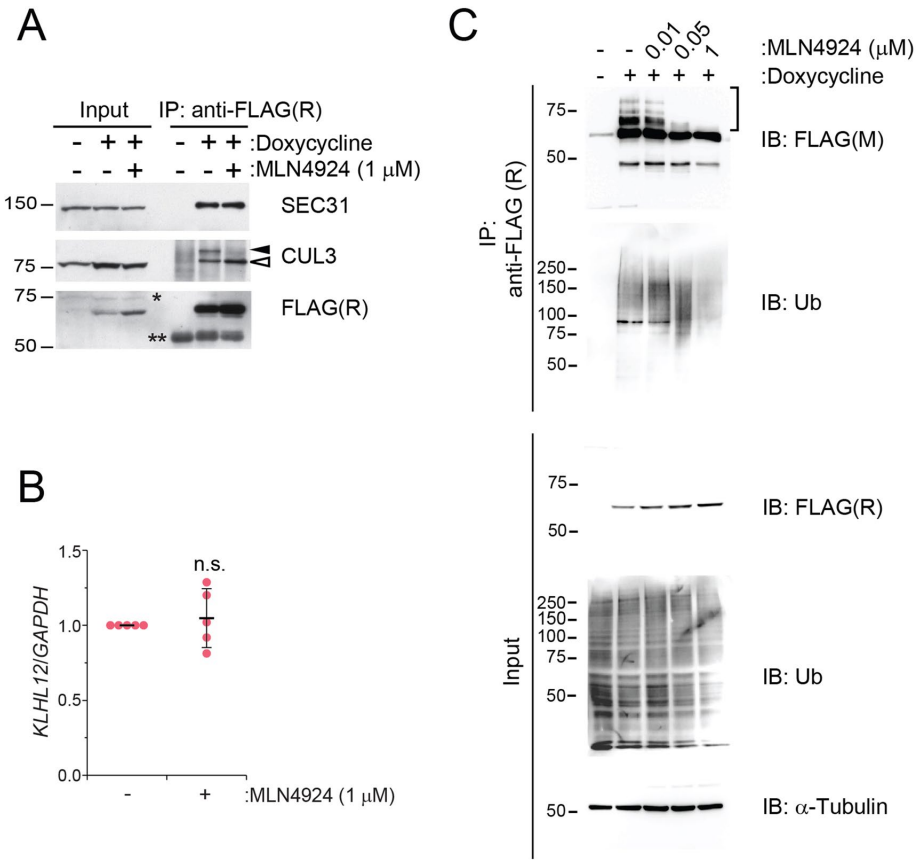

FIGURE 1: MLN4924, an inhibitor of NEDD8-activating enzyme, inhibits the ubiquitylnation of KLHL12. Flp_In T-REx 293 cells stably expressing KLHL12–FLAG were treated with or without MLN4924 for 24 h. Expression of KLHL12–FLAG was induced with doxycycline (1 μg/ml) for 24 h. (A, C) Cellular lysates were processed for coimmunoprecipitation using a rabbit (R) or a mouse (M) anti-FLAG antibody. The mouse anti-FLAG antibody detected slowly migrating KLHL12–FLAG species better than the rabbit anti-FLAG antibody. These species disappeared as the MLN4924 concentration increased. We suspect that these species are polyubiquitylated KLHL12. Closed arrowhead, neddylated CUL3; open arrowhead, unneddylated CUL3. *Nonspecific band. **Immunoglobulins. (B) Levels of *KLHL12* mRNAs were measured with RT-qPCR and were normalized to those of *GAPDH* mRNAs. Statistical analysis was performed with Student's *t*-test ($n = 5$). Error bars represent SD. The primer information is shown in Supplemental Table S2.

and membrane proteins destined to cellular locations. Collagens are the major component of the extracellular matrix (ECM). Type I and II procollagens form about 300 nm–long rigid triple helices (Bachinger *et al.*, 1993; Bonfanti *et al.*, 1998) and require COPII proteins for ER export (Boyadjiev *et al.*, 2006; Townley *et al.*, 2008; Long *et al.*, 2010; Ohisa *et al.*, 2010; Sarmah *et al.*, 2010; Garbes *et al.*, 2015; Zhu *et al.*, 2015; Lu and Kim, 2020; Lu *et al.*, 2022). Because COPII proteins typically generate vesicles 60–80 nm in diameter, a mechanism must exist that allows COPII coat proteins to accommodate such large cargo molecules. Alternatively, a COPII-dependent short-loop pathway that does not involve large vesicles may account for the transport of procollagen from the ER to the Golgi (McCaughey *et al.*, 2018). Recently, live-cell imaging of GFP-tagged endogenous procollagens has shown that ARF1-dependent transport intermediates deliver procollagen from ER exit sites (ERESs) to the Golgi, suggesting that vesicular carriers deliver procollagens from the ER to the Golgi (Gorrell *et al.*, 2021). Thus, it remains elusive if and how large COPII structures contribute to ER export of procollagen.

When KLHL12 was overexpressed, larger COPII-coated vesicles (>500 nm) were observed (Jin *et al.*, 2012) and collagens were found in the large structures coated with COPII and KLHL12 (Gorur *et al.*, 2017). In addition, the large COPII structures were generated even in the presence of lysine-free ubiquitin, which prevents polyubiquitylation of SEC31 (Jin *et al.*, 2012). Thus, the Ub ligase activity of $CRL3^{KLHL12}$ seems to be critical for enlarging COPII vesicles through monoubiquitylation of SEC31. Although $CRL3^{KLHL12}$ is an Ub ligase, cullin itself is not a catalytic subunit, but serves as a scaffold. The Ub ligase activity of CRL3s is known to be activated by CUL3 neddylation, as CUL3 neddylation induces a conformational change near the RBX1 binding region (Merlet *et al.*, 2009). This conformational change results in juxtaposition of E2-Ub to a substrate (Petroski and Deshaies, 2005b; Saha and Deshaies, 2008). Consistent with this idea, defects in the neddylation pathway phenocopies the inactivation of CUL3 in *Caenorhabditis elegans* (Kurz *et al.*, 2002). In this study, we tested the role of CUL3 neddylation in large COPII vesicle assembly in cultured cells.

RESULTS AND DISCUSSION

MLN4924 is a potent inhibitor of CRL3s

MLN4924 is a potent inhibitor of NEDD8-activating enzyme and strongly inhibits the catalytic activity of CRLs (Soucy *et al.*, 2009). To test its role in the assembly of large COPII-KLHL12 structures, we established a doxycycline-inducible Flp_In T-REx 293 cell line stably expressing FLAG-tagged KLHL12 (KLHL12–FLAG). The effective concentration range of MLN4924 for the inhibition of CUL neddylation was 0.01–1 μM (Supplemental Figure S1A and Figure 1A). Unexpectedly, we observed an increase of KLHL12 levels upon inhibitor treatment (Supplemental Figure S1A and Figure 1A). This increase was not caused by an increased expression of *KLHL12* (Figure 1B). Endogenous KLHL12 levels were increased by MLN4924 treatment in human U-2 osteosarcoma (U2OS) cells, too (Supplemental Figure S1B). This increase of endogenous KLHL12 levels was not caused by an increased expression of endogenous *KLHL12* (Supplemental Figure S1C). When we immunoprecipitated KLHL12, SEC31 and CUL3 were coprecipitated in the presence of the inhibitor (Figure 1A, IP), suggesting that MLN4924 does not disrupt the interaction of KLHL12 with CUL3 and SEC31.

We then asked if MLN4924 can affect the ubiquitylation activity of CRL3s. However, ubiquitylated forms of endogenous SEC31 were not detectable under our experimental conditions or under the conditions used by Jin *et al.* (2012). To circumvent this problem, we took advantage of the observation that the levels of KLHL12 were increased by an MLN4924 treatment (Figure 1A). It has been reported that an MLN4924 treatment increased KLHL3 levels by inhibiting CUL3-dependent KLHL3 polyubiquitylation (McCormick *et al.*, 2014).

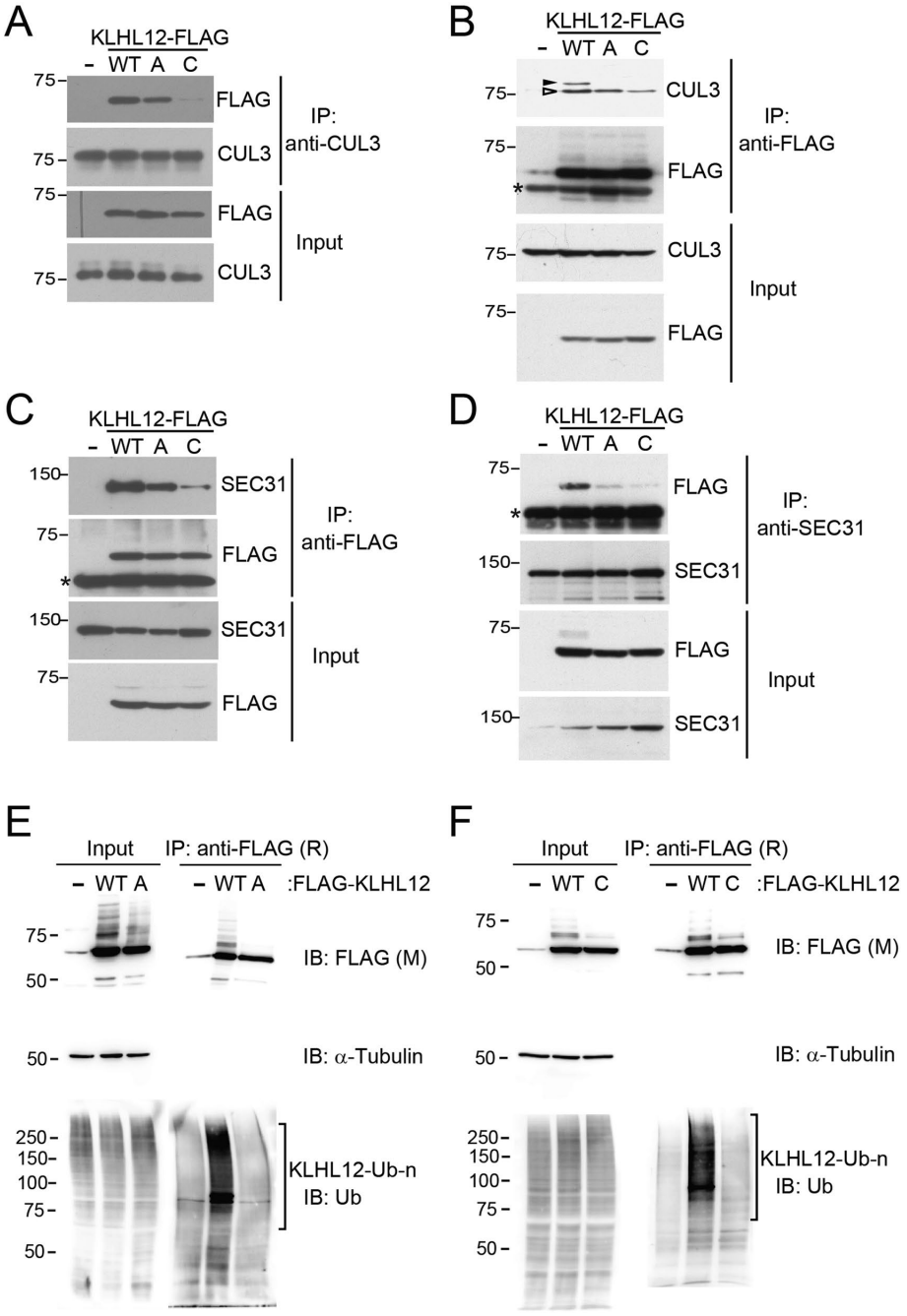

FIGURE 2: The KLHL12-CUL3 interaction influences the KLHL12–SEC31 interaction. (A–D) Stable Flp_In T-REx 293 cells harboring an empty vector (—) or an indicated KLHL12–FLAG construct were treated with doxycycline (1 μg/ml) for 24 h to induce the expression of a KLHL12–FLAG construct. Cellular lysates were processed for immunoprecipitation using an indicated antibody. (E and F) Cellular lysates of Flp_In T-REx 293 cells stably expressing KLHL12 wild type or Mut A or Mut C were processed for immunoprecipitation using an anti-FLAG antibody. A mouse anti-FLAG antibody was used to probe KLHL12. The closed arrowhead and the open arrowhead represent neddylated and unneddylated CUL3, respectively. *Immunoglobulin. WT, wild type; A, Mut A; C, Mut C.

Similarly, CUL3 may polyubiquitylate KLHL12. If this is the case, MLN4924 would inhibit KLHL12 ubiquitylation, accounting for the increase in KLHL12 levels. To test this idea, we probed for KLHL12 ubiquitylation. Indeed, MLN4924 treatments inhibited the ubiquitylation of KLHL12 (Figure 1C, Ub panels). Thus, this result raises the possibility that CUL3 regulates the levels of KLHL12 through polyubiquitylation.

KLHL12 ubiquitylation is CUL3-dependent

To test if KLHL12 ubiquitylation is CUL3-dependent, we generated KLHL12 constructs with mutations at the KLHL12–CUL3 interface (Supplemental Figure S2; Mut B was not expressed for unknown reasons). Mut A or Mut C showed a varying degree of defects in CUL3 binding (Figure 2, A and B). In addition, we noticed a strong reduction of neddylated (ned) CUL3 bound to Mut A or Mut C (Figure 2B). This was not due to lack of ned-CUL3 in the cell, as we observed ned-CUL3 in total cell lysates prepared from cells stably expressing the KLHL12 variants (Supplemental Figure S3). Mut A and Mut C also showed varying degrees of defects in SEC31 binding (Figure 2, C and D). Clearly, the KLHL12–CUL3 interface is important not only for KLHL12–CUL3 interaction, but also for KLHL12–SEC31 interaction. We then tested if these KLHL12 variants show defects in KLHL12 ubiquitylation (Figure 2, E and F). Unexpectedly, the ubiquitylation of Mut A was drastically reduced while that of Mut C was reduced to a lesser degree (see Ub panel). Perhaps Mut C is misfolded in such a way that it triggers ubiquitylation by other E3 ubiquitin ligase. Mut C immunofluorescent labeling suggests a conformation change in Mut C (see Figure 3B). These results support the idea that KLHL12 ubiquitylation depends on proper CUL3 interaction. In addition, Mut A still interacts with CUL3 and SEC31 to a reduced degree, but fails to form a functional ligase with CUL3. Our data indicate that KLHL12 ubiquitylation is CUL3–dependent.

Persistent formation of COPII–KLHL12 structures without CUL3 neddylation

We then asked whether MLN4924 could block the formation of large/exaggerated COPII-coated structures. To test this possibility, we treated the Flp_In T-REx 293 cells stably expressing KLHL12 with MLN4924 and monitored COPII–KLHL12–coated structures via immunofluorescent microscopy. In the absence of doxycycline, only background signals were observed for KLHL12 (Supplemental Figure S4). As previously reported, the overexpression of KLHL12 induced formation of large COPII–KLHL12–coated structures (Figure 3A, DMSO panel; Gorur *et al.*, 2017; Jin *et al.*, 2012). Interestingly, even though we used a high concentration of MLN4924 (1 μM), we observed apparently normal-looking large structures (Figure 3, A and C, MLN4924 panels, closed arrowheads). In the presence of MNL4924, we also observed aberrant COPII–KLHL12 structures

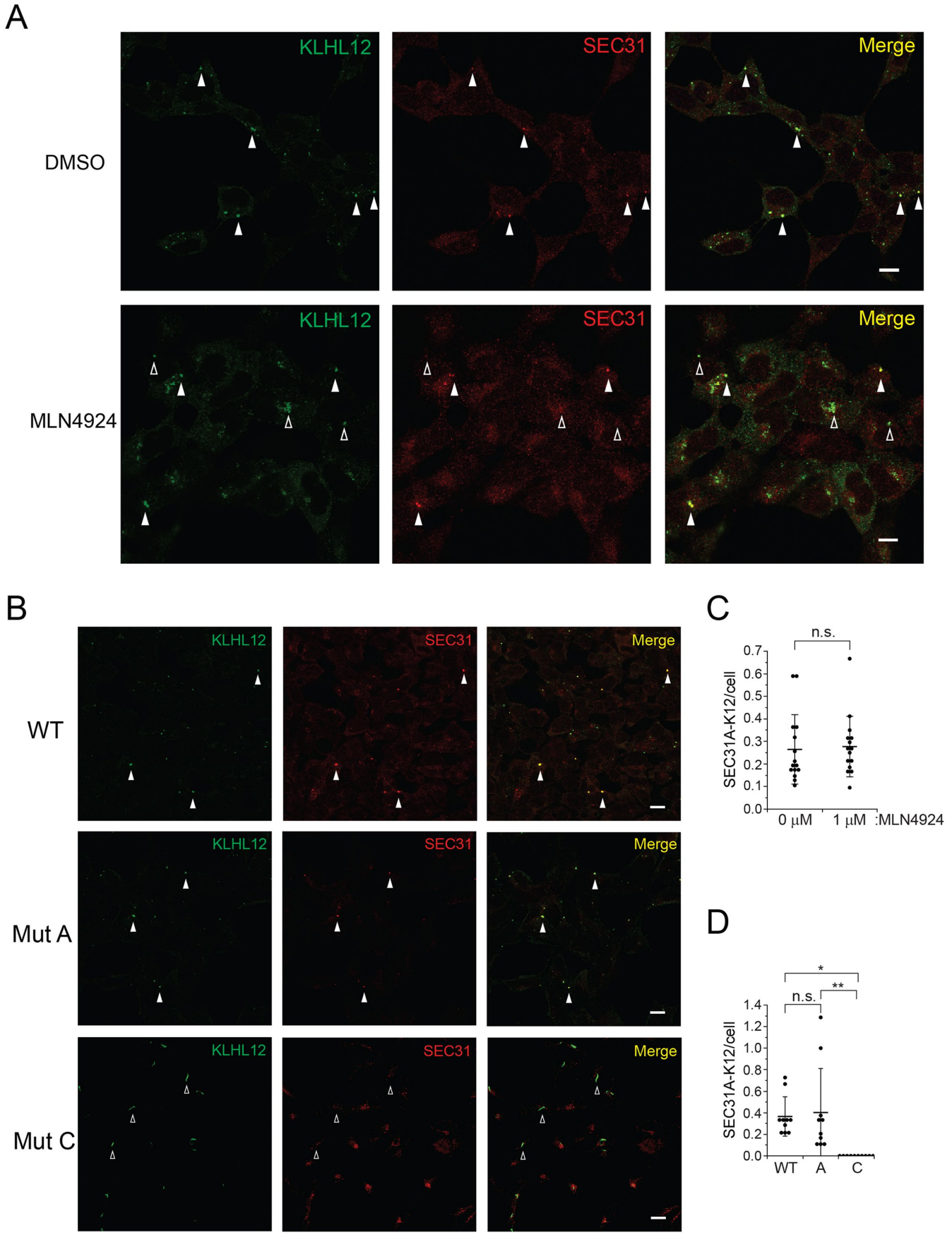
A
KLHL12
SEC31
Merge
DMSO
MLN4924
B
WT
Mut A
Mut C
C
n.s.
SEC31A-K12/cell
0 μM
1 μM
:MLN4924
D
*
**
n.s.
WT
A
C

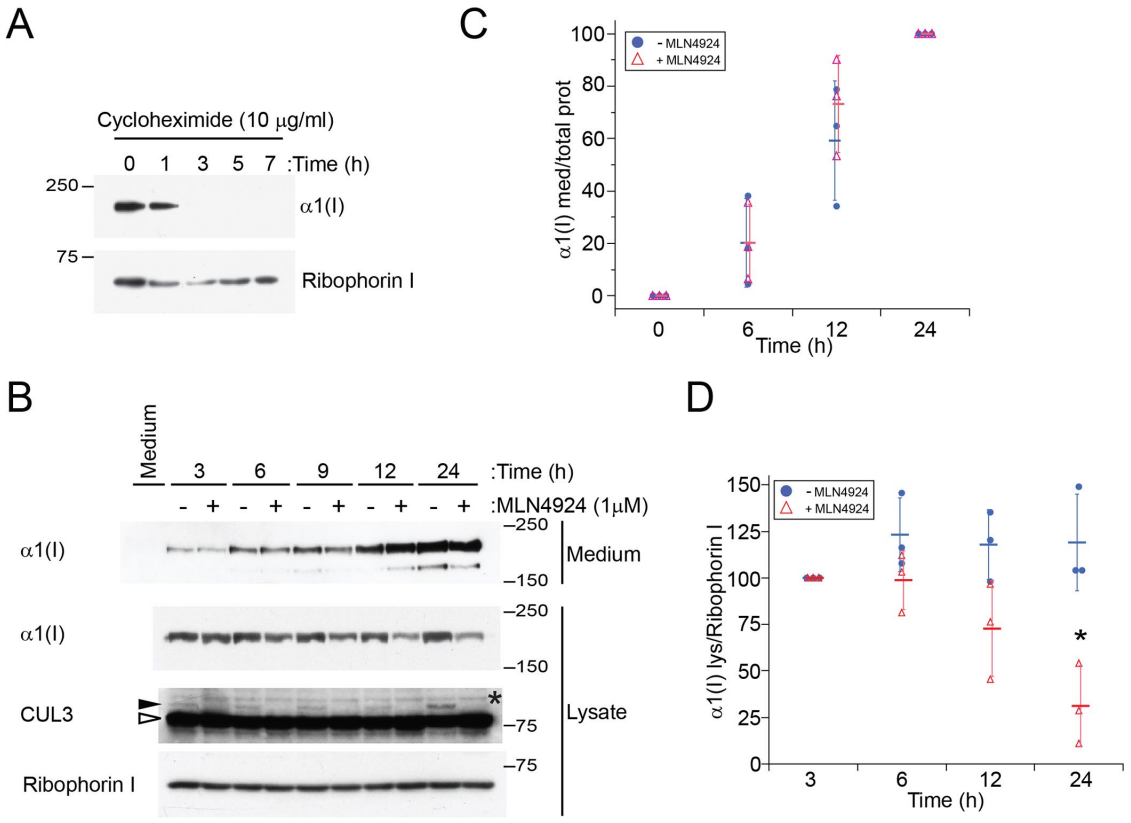

FIGURE 4: Regulation of cellular type I collagen α1, α1(I), levels by MLN4924. (A) A rapid depletion of cellular collagens was observed in human skin fibroblasts (HSFs) after cycloheximide treatment. (B) HSFs were plated and incubated for 24 h. Afterward, the culture medium was replaced with fresh medium with or without MLN4924 (1 μM). Conditioned media and cells were collected at indicated times and processed for immunoblotting. The amount of medium loaded into the gel was normalized to the amount of total proteins in a cell lysate. Riboporin I was probed as a loading control. Medium, unconditioned medium; closed arrowhead, ned-CUL3; open arrowhead, unneddylated CUL3. Note that neddylated CUL3 is visible only when the film was overexposed. (C, D) Quantification of levels of collagen in the media (C) and lysates (D). Error bars represent standard deviations and middle bars averages. Protein bands were quantified using ImageJ. Student's *t*-test: $*p < 0.005$, $n = 3$.

with reduced SEC31 signals (Figure 3A, MLN4924 panels, open arrowheads). Perhaps the increased levels of KLHL12 in MLN4924-treated cells exceed the capacity for assembly of normal COPII structures, leading to aberrant assembly. Regardless, large COPII–KLHL12 structures persisted even in the absence of ned-CUL3. It is striking that even though MLN4924 has a broad range of inhibitory activities, it does not prevent the formation of large/exaggerated COPII-KLHL12 structures.

To test if KLHL12 can support the formation of COPII–KLHL12 structures when KLHL12 is expressed at lower levels, we stably expressed a Tet-inducible KLHL12–FLAG construct in U2OS cells. In the absence of doxycycline, only background signals were observed for KLHL12 (Supplemental Figure S5G). At 1-ng/ml doxycycline concentration, recombinant *KLHL12* were modestly overexpressed (Figure 5E). Under this condition, we observed small COPII–KLHL12 structures (Supplemental Figure S5, A and B). This is consistent with a

FIGURE 3: Large COPII structures with unneddylated $CRL3^{KLHL12}$. (A) Flp_In T-REx 293 cells stably expressing WT KLHL12–FLAG were incubated in the presence (1 μM) or absence (DMSO) of MLN4924 and processed for immunofluorescent labeling. Labeled cells were visualized by standard confocal microscopy. KLHL12 expression was induced with 1 μg/ml doxycycline for 24 h. (B) Flp_In T-REx 293 cells stably expressing the indicated construct were processed for immunofluorescent labeling. Labeled cells were visualized by standard confocal microscopy. Large structures that are costained with KLHL12 and SEC31A were marked with closed arrowheads. Those that are deficient of SEC31A labeling were marked with open arrowheads. (C, D) Areas of KLHL12 punctate structures that are positive for SEC31A were measured with the particle analysis of ImageJ. Diameters were calculated based on the assumption that the structures are round. Structures that are larger than 250 nm in diameter were counted. (C) Comparison between the untreated (440 cells from 15 micrographs) and MLN4924-treated (288 cells from 15 micrographs). We used Student's *t*-test for statistical analysis. n.s., not significant. (D) Comparison between wild-type KLHL12 (73 cells from 10 micrographs), Mut A (74 cells from 10 micrographs), and Mut C (84 cells from 10 micrographs). Scale bars, 10 μm. We used one-way ANOVA with Tukey's correction for multiple comparisons. Mut A and Mut C were compared with WT (* $p < 0.05$) and Mut A was also compared with Mut C (** $p < 0.01$). n.s., not significant.

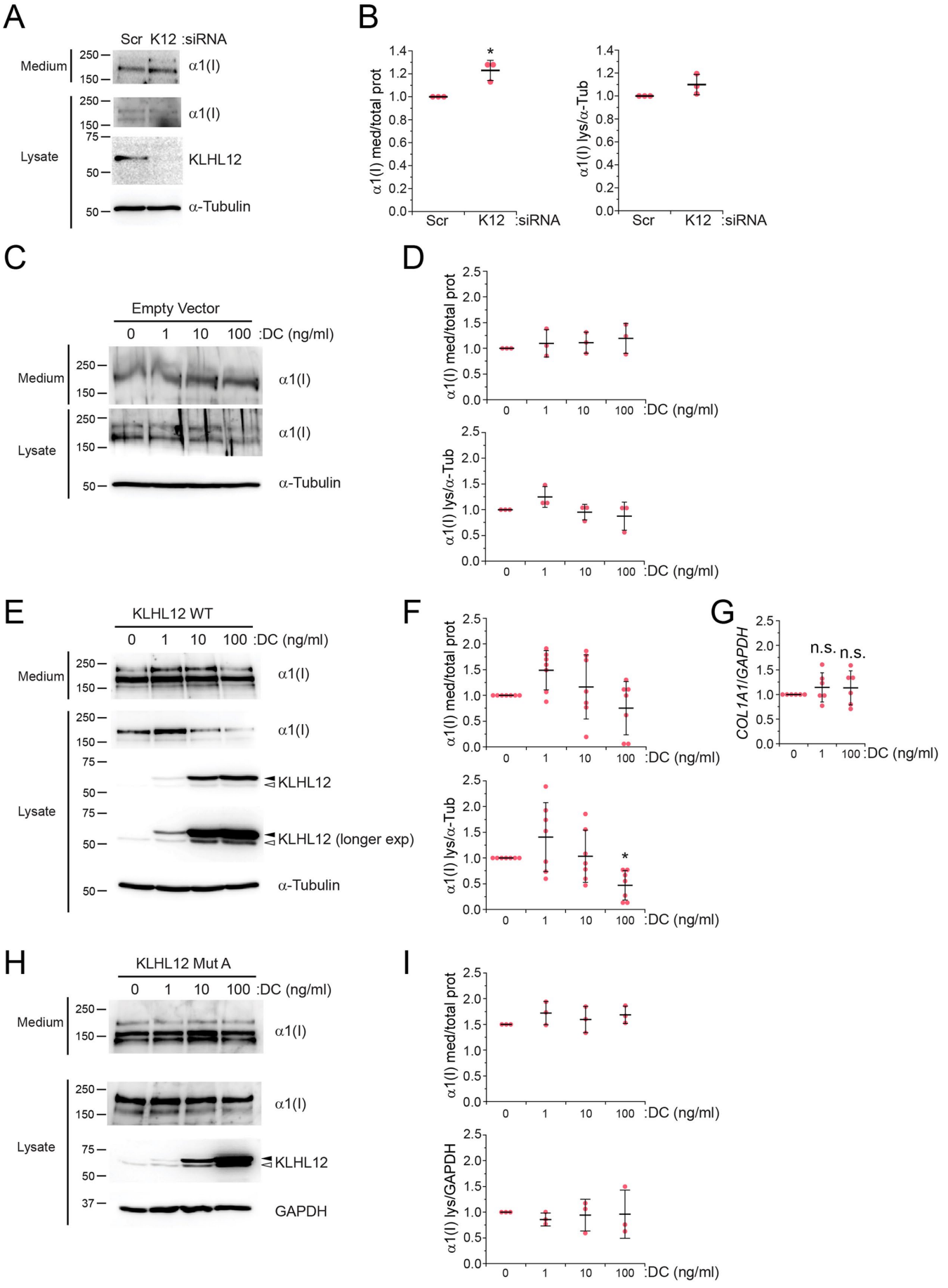
A
Scr K12 :siRNA
Medium
Lysate
250
150
75
50
α1(I)
α1(I)
KLHL12
α-Tubulin
B
α1(I) med/total prot
α1(I) lys/α-Tub
Scr K12 :siRNA
C
Empty Vector
0 1 10 100 :DC (ng/ml)
D
:DC (ng/ml)
E
KLHL12 WT
KLHL12
KLHL12 (longer exp)
F
G
COL1A1/GAPDH
n.s.
H
KLHL12 Mut A
37
GAPDH
I
α1(I) lys/GAPDH

previous result that a pool of KLHL12 is found in COPII-positive punctate structures (Omari *et al.*, 2018). Interestingly, we no longer observed large COPII–KLHL12 structures (Supplemental Figure S5, A and B), consistent with the observation that large/exaggerated COPII–KLHL12 structures are observed when KLHL12 is overexpressed (Jin *et al.*, 2012). When the cells were also treated with MLN4924, large COPII–KLHL12 structures were observed (asterisks in Supplemental Figure S5, C–E). This is likely because KLHL12 is stabilized by MLN4924 treatment, resulting in higher KLHL12 levels (Figure 1A and Supplemental Figure S1B). Clearly, MNL4924 treatment does not interfere with the formation of COPII–KLHL12 structures.

As Mut A and Mut C failed to form a stable complex with neddCUL3 and Mut A is not ubiquitylated by CUL3, we asked if they still support the assembly of large COPII–KLHL12 structures (Figure 3, B and D). Mut A induced the formation of apparently normal COPII–KLHL12 structures and Mut C induced the formation of elongated KLHL12 structures. SEC31 fluorescence was detectable in Mut A structures, but not in Mut C structures, consistent with our immunoprecipitation results (Figure 2, C and D). Taken together, our data suggest that CUL3 neddylation or KLHL12 ubiquitylation is not necessary for the formation of COPII–KLHL12 structures. This result is consistent with the result obtained from MLN4924-treated cells.

MLN4924 reduces cellular collagen levels

MLN4924 treatment inhibits CUL3 neddylation potently, but not the formation of large COPII–-KLHL12 structures. We were curious how this inhibitor affects collagen secretion. We used human skin fibroblasts (HSFs), which secrete type I collagen robustly, because the Flp_In T-REx 293 cells that derived from HEK293 cells do not express type I collagen (Supplemental Figure S6). Intracellular collagen molecules were efficiently depleted within 3 h in HSFs when new collagen synthesis was blocked (Figure 4A). Notably, the proteolytic processing of collagen propeptides occurs in the Golgi and in the extracellular space, but this process is inefficient in cultured cells (Canty and Kadler, 2005), probably because the collagen processing factors are diluted in the culture medium. Thus, even procollagens are detectable in the culture medium. The secretion of collagen was not reduced during the 24 h period of MLN4924 treatments (Figure 4, B and C). Unexpectedly, the levels of intracellular collagen were reduced by the inhibitor treatments during this period (Figure 4, B and D). Intracellular collagen was undetectable with prolonged MLN4924 treatments (Supplemental Figure S7 [Lysate panel: compare the 24 h (+) with 48 h (+)]). Under this prolonged treatment condition, we observed no additional increase of collagen deposition in the medium in the presence of the inhibitor (Medium panel: compare the 24 h (+) with 48 h (+)). We observed, however, an increased deposition of collagen in the medium in the absence of the inhibitor (Medium panel: compare the 24 h (–) with 48 h (–)). Thus, MLN4924 reduces intracellular collagen levels and eventually leads to reduced collagen secretion. These data suggest that the neddylation of CRL3s is critical for the maintenance of cellular collagen levels.

KLHL12 affects the levels of α1(I)

Although it was interesting to see that MLN4924 affects cellular collagen levels, this could be ascribed to various activities of cullins, as MLN4924 inhibits a broad range of cellular activities involving NEDD8-activating enzyme (Soucy *et al.*, 2009). For example, CUL3 can possibly work with 183 BTB-domain proteins, including proteins with Kelch domains, to ubiquitylate diverse substrates (Stogios *et al.*, 2005). To test if KLHL12 can affect collagen levels, we altered the levels of KLHL12 with RNA interference (RNAi) or with a controlled expression of recombinant *KLHL12–FLAG* in U2OS cells. KLHL12 depletion with a small interfering RNA (siRNA) targeting 3′UTR resulted in only a slight (about 20%) increase in secreted collagen levels (Figure 5, A and B). Probably other KLHL proteins share a redundant function with KLHL12 or a compensatory mechanism is activated when KLHL12 is depleted. We then tested if overexpression of a recombinant *KLHL12* affects collagen secretion. As a control, we used U2OS cells stably transfected with the empty vector. Collagen levels did not change after doxycycline treatment when the cells harbored an empty vector (Figure 5, C and D). As excessive recombinant *KLHL12* was expressed, we observed about 50% reduction of intracellular collagen levels without significant effect on secreted collagen levels. The changes in collagen levels were not consequences of decreased *COL1A1* mRNA levels (Figure 5G). A bafilomycin A1 treatment stabilized collagen levels, and this stabilization was more evident when *KLHL12* was highly overexpressed (Supplemental Figure S8). Thus, it seems that when KLHL12 levels are excessive, more collagen molecules are sent to lysosomes for degradation. Overexpression of Mut A did not affect collagen levels (Figure 5, H and I), suggesting that the Ub ligase activity of $CRL3^{KLHL12}$ is necessary to stimulate lysosomal degradation of collagen.

FIGURE 5: KLHL12 affects α1(I) levels. KLHL12 levels were modulated with KLHL12 siRNAs or by introducing a recombinant KLHL12–FLAG construct (Tet-inducible) to U2OS cells. (A, B) U2OS cells were transfected with scrambled (Scr) siRNAs or KLHL12 (K12) siRNAs targeting 3′UTR (50 nM) for 48 h and media were replaced with fresh media. The cells and the conditioned media were collected after an additional 24 h of incubation. (A) Representative immunoblot images. Scr, scrambled. K12, KLHL12. DC, doxycycline. (B) Comparison of α1(I) levels in the cell lysates and in the media. Immunoblots images of three independent experiments were quantified with ImageJ. Statistical analyses were performed with Student's *t*-test. Error bars represent standard deviations. Cellular α1(I) was normalized to α-tubulin and secreted α1(I) was normalized to total cellular proteins. *$p < 0.01$, $n = 3$. (C–I) U2OS cells harboring an empty vector (C and D), KLHL12 WT (E–G), and KLHL12 Mut A (H and I), were incubated with doxycycline as indicated for 48 h. Then, the cells and the conditioned media were collected. (C) Representative immunoblot images. (D) Comparison of α1(I) levels in the cell lysates and in the media. Statistical analysis was performed with Student's *t*-test ($n = 3$). No statistically significant changes were observed, compared with 0 ng doxycycline. (E) Representative immunoblot images. Closed arrowhead, recombinant KLHL12-FLAG; open arrowhead, endogenous KLHL12. (F) Comparison of α1(I) levels in the cell lysates and in the media. Statistical analysis was performed with Student's *t*-test. *$p < 0.0005$, $n = 7$. (G) Levels of *COL1A1* mRNAs were measured with RT-qPCR and were normalized to those of *GAPDH* mRNAs. Statistical analysis was performed with Student's *t*-test ($n = 6$). Error bars represent SD. The primer information is shown in Supplemental Table S2. (H) Representative immunoblot images. (I) Comparison of α1(I) levels in the cell lysates and in the media. Statistical analysis was performed with Student's *t*-test ($n = 3$). No statistically significant changes were observed, compared with 0 ng doxycycline.

Our observation is consistent with a report that some procollagen molecules are rerouted to lysosomal degradation and KLHL12 is found in the COPII/autophagic marker-positive punctate structures (Omari *et al.*, 2018). It is unclear why excessive KLHL12 expression resulted in a reduction in intracellular collagen levels. Perhaps when *KLHL12* is expressed excessively, surplus KLHL12s stimulate rerouting of procollagens to lysosomes. LUNAPARK (LNP) is an ER membrane protein which can recruit and inactivate KLHL12 (Akopian *et al.*, 2022; McGourty *et al.*, 2016). The PEF1–ALG2 complex releases KLHL12 from LNP in a Ca^{2+}-dependent manner and recruits its substrate (e.g., SEC31A) to assemble substrate-bound $CRL3^{KLHL12}$. $CRL3^{KLHL12}$ and then monoubiquitylates PEF1 to stabilize the ligase for efficient substrate modification. If LNP inhibits KLHL12 to regulate collagen levels, depletion of LNP is expected to free up KLHL12, resulting in lysosomal degradation of collagen. When we depleted LNP, however, collagen levels were not affected (Supplemental Figure S9). Thus, LNP–KLHL12 interaction does not seem to be critical for collagen degradation. In addition, ALG2-to-PEF1 ratio is suggested to play a role in protein secretion (Sargeant *et al.*, 2021). Under our conditions, levels of ALG2 and PEF1 or the ratio of ALG2 to PEF1 did not change (Supplemental Figure S10). The exact mechanism about how KLHL12 affects collagen degradation remains to be determined. Our data clearly indicate that KLHL12 is involved in maintaining cellular collagen levels, rather than that it affects the transport of procollagen directly from the ER to the Golgi.

CUL3 neddylation is critical for the Ub ligase activity of CRL3 (Merlet *et al.*, 2009). Here, we inhibited the neddylation of CUL3 with MLN4924. In addition, by introducing mutations at the KLHL12–CUL3 interface, we generated KLHL12 mutants that are unable to form a complex with ned-CUL3. Despite the mutations and MLN4924 treatment, large COPII–KLHL12 structures persisted. In addition, small COPII–KLHL12 structures persisted in the presence of MLN4924. Thus, our data suggest that CUL3 neddylation is not necessary for the assembly of COPII–KLHL12 structures. While our data do not support the existing model that $CRL3^{KLHL12}$ monoubiquitylates SEC31 to promote the formation of large COPII structures and expedites collagen secretion, our results are consistent with the observations that lysine-free Ub supports the formation of the large structures and mutations at the expected ubiquitylation sites of SEC31A did not prevent large structure formation (Jin *et al.*, 2012). These two observations agree with our model that the ligase activity of $CRL3^{KLHL12}$ is not necessary for the formation of large structures.

Importantly, we found that overexpressed KLHL12 can lower intracellular collagen levels, probably through ER-to-lysosomal pathways, and Mut A fails to do so, suggesting that active $CRL3^{KLHL12}$ is necessary to stimulate lysosomal targeting of collagen. The role of KLHL12 in lysosomal degradation of collagen is also consistent with the observation that KLHL12 is found in some ER exit sites where autophagic markers are present (Omari *et al.*, 2018). In conclusion, our results suggest that KLHL12 plays a role in maintaining collagen levels through the ER-to-lysosome pathway rather than the ER-to-Golgi pathway. However, as KLHL12 depletion only modestly increased secreted collagen levels and excessive expression of *KLHL12* lowered collagen levels, it does not appear that KLHL12 is critical for the regulation of collagen levels at its physiological levels. Perhaps other KLHL proteins share a redundant function with KLHL12 for this activity.

MATERIALS AND METHODS

Request a protocol through *Bio-protocol*.

Plasmid and siRNA

The pcDNA5/FRT/TO KLHL12-FLAG construct was a gift of Michael Rape's laboratory (University of California, Berkeley, CA). The KLHL12 Mut A (ELSE65-68AAAA), Mut B (CLLQLK111-116AAAAAA), and Mut C (FAETHNC141-147AAAAAAA) were generated by site-directed mutagenesis (Supplemental Figure S2 and Supplemental Table S1). pCMV6-Entry (PS100001), human pCMV6-KLHL40-Myc-DDK (RC213832), and human pCMV6-KLHL41-Myc-DDK (RC200295) were purchased from Origene (Rockville, MD). The pLVX-TRE3G and pLVX-Tet3G constructs used to clone KLHL12 were purchase from Takara Bio USA as part of the In-Fusion HD Cloning Kit (121416). The controls (D-001206-13) were purchased from Dharmacon (Lafayette, CO). Sequences of these siRNAs are as follows. Control (pool of 4) siRNAs: 5′-UAGCGACUAAACACAUCAA-3′, 5′-UAAGGCUAUGAAGAGAUAC-3′, 5′-AUGUAUUGGCCUGUAUUAG-3′, 5′-AUGAACGUGAAUUGCUCAA-3′. KLHL12 (3′UTR): 5′-UGACAGUAGCCUAGUAGUUUU-3′.

Antibodies and chemicals

Rabbit anti-α1(I) antibodies were a gift from L. Fisher (LF-68, 1:8000, National Institute of Dental and Craniofacial Research, Bethesda, MD; Fisher *et al.*, 1995) or purchased from Kerafast (ENH018-FP, Boston, MA). Rabbit anti-ribophorin I antibody (1:5,000) was a gift from the Schekman laboratory (University of California, Berkeley, CA). Additional antibodies we used include rabbit anti-CUL3 (A301-109A, 1:1000, Bethyl Laboratories, Universal Biologicals, Cambridge, UK), mouse FK2 anti-Ub (BML-PW8810, 1: 1000, Enzo Life Sciences, Farmingdale, NY), anti-FLAG (F3165, F7425, 1:1500, Sigma-Aldrich, St. Louis, MO), anti-ubiquitin (P4D1; 14049, 1:1000, Cell Signaling Technology, Danvers, MA), mouse anti-KLHL12 (#30058, 1:1000, ProMab Biotechnology, Richmond, CA), anti-SEC31A (#612350, BD Biosciences, San Diego, CA; A302-336A, Bethyl Laboratories, Universal Biologicals, Cambridge, UK), and monoclonal anti-α-tubulin (TU-02, sc-8035, 1:2000, Santa Cruz Biotechnology, Dallas, TX). Hygromycin B (10687-010) and blasticidin S (R210-01) were purchased from Invitrogen (Carlsbad, CA). Cycloheximide (CHX, C4859), dimethyl sulfoxide (DMSO, D4540,) and 1, 4-dithiothreitol (DTT, D0632) were purchased from Sigma-Aldrich (St. Louis, MO). Puromycin dihydrochloride was purchased from Millipore Sigma (540222). Normocin was purchased from InvivoGen (ant-nr-1, San Diego, CA). Protease inhibitor cocktail (Mannheim, Germany), MLN4924 (15217, Cayman Chemical, Ann Arbor, MI), MG132 (474790, Calbiochem, San Diego, CA), and brefeldin A (BFA, #9972, Cell Signaling Technology, Danvers, MA) were also used.

Cell culture and transfection

Normal human skin fibroblasts (CRL-2091), HeLa cells (HeLa, CCL-2), and human U-2 osteosarcoma (U2OS, HTB-96TM) were purchased from the American Type Culture Collection (ATCC, Manassas, VA). Cells were maintained in low-glucose DMEM with 10% fetal bovine serum (FBS) and 1% penicillin–streptomycin. In the case of U2OS cells, they were maintained in McCoy's 5A medium with 10% fetal bovine serum (FBS), 1% penicillin–streptomycin, and 100 μg/ml normocin. U2OS cells stably expressing *KLHL12* were grown in growth medium with G418 (0.8 mg/ml) and puromycin (2.8 μg/ml). *KLHL12* expression was induced by 0.001–0.1 μg/ml doxycycline in U2OS cells. Flp_In T-REx™ 293 host cell line containing a stably integrated FRT site and tetracycline (Tet) repressor was grown in high-glucose DMEM, supplemented with 10% FBS, blasticidin, and hygromycin B as instructed by the manufacturer (Life Technologies/Thermo Fisher, Waltham, MA), and gene

expression was induced by 1 μg/ml doxycycline. Cells were maintained in high-glucose DMEM with 10% FBS and 1% penicillin–streptomycin for proliferation (Life Technologies/Thermo Fisher, Waltham, MA). Cell lines were maintained in a water-jacketed incubator at 37°C with 5% CO_2 enrichment. Lipofectamine LTX 3000 was used for plasmid DNAs transfection, Lipofectamine RNAiMAX for siRNAs transfection, and Lenti-X Tet-One Inducible Expression Systems for lentiviral transfection according to the manufacturer's protocols unless specified otherwise. All of the cell culture and transfection reagents were purchased from Invitrogen (Carlsbad, CA) or Takara Bio USA (Mountain View, CA).

Establishing stable cell lines

Flp-In T-REx 293 cells stably expressing Tet-inducible KLHL12 WT, Mut A, and Mut C were generated according to the manufacturer's instructions (Flp-In System, Invitrogen, Carlsbad, CA). Briefly, the Flp-In T-REx 293 Cells (R780-07) were plated onto 6-well plates and incubated for 24 h. The following day, the cells were transfected using 5 μl lipofectamine LTX with 0.5 μg of a KLHL12 construct and 1.0 μg of pOG44 (V6005-20). At 48 h posttransfection, the cells were replated on 24-well plates and subjected to selection with hygromycin B (100 μg/ml) and blasticidin S (10 μg/ml) for up to 4 wk. When indicated, 1 μg/ml doxycycline was used to induce the expression of KLHL12 in this cell line.

U2OS cells stably expressing Tet-inducible *KLHL12–FLAG* were generated according to the manufacturer's instructions (Lenti-X Tet-One Inducible Expression Systems, Takara Bio USA, Mountain View, CA). U2OS cells were plated onto 6-well plates and incubated for 24 h. The following day cells were transfected using pLVX-Tet3G and pLVX-TRE3G-KLHL12 lentiviral stocks using 1:3:3 MOI ratio (cell density:Tet3G:TRE3G-KLHL12). Polybrene at final concentration of 4 μg/ml was used in combination with centrifugation (1200 × *g* for 90 min at 32°C) to improve transfection efficiency. After 24 h transduction, virus-containing medium was removed and replaced with fresh growth medium. Cells were incubated for an additional 48 h before they were subjected to selection with G418 (0.8 mg/ml) and puromycin (2.8 μg/ml).

Coimmunoprecipitation and immunoblotting

For coimmunoprecipiation, cells were collected by centrifugation and lysed by douncing 30 times using buffer A (0.1% NP-40, 2.6 mM KCl, 1.5 mM KH_2PO_4, 140 mM NaCl, 8 mM Na_2HPO_4-·$7H_2O$, and 1X protease inhibitor cocktail) on ice. After centrifugation for 15 min at 14,000 rpm at 4°C, cleared lysates were incubated in the cold room with indicated antibodies overnight, followed by incubation with protein A or protein G Sepharose beads (GE Healthcare, Milwaukee, WI) for 3 h with gentle rocking in the cold room. The beads were harvested by centrifugation and washed three times with buffer A. After the SDS-sample buffer was added and they were heated for 5 min at 95°C, proteins were resolved with SDA–PAGE and processed for immunoblotting.

For routine immunoblotting analysis, cells were lysed with buffer B (20 mM Tris-HCl, pH 7.5, 150 mM NaCl, 1 mM Na_2EDTA, 1 mM EGTA, 1% NP-40, 1% sodium deoxycholate, 2.5 mM sodium pyrophosphate, 1 mM β-glycerophosphate, 1 mM Na_3VO_4, 1X complete protease inhibitor cocktail) on ice for 15 min. Cell lysates were cleared by centrifugation at 14,000 rpm for 15 min at 4°C. Cleared lysates were quantified using Pierce BCA Protein Assay Kit (Thermo Fisher Scientific, Waltham, MA). Equal amounts of proteins were resolved on 6%, 8%, or10% SDS–PAGE, transferred to PVDF membrane (Millipore, Bedford, MA), probed with primary antibodies and subsequently with horseradish peroxidase–conjugated secondary antibodies, and visualized with ECL Prime (GE Healthcare, Pittsburgh, PA). Band intensity was quantified using the ImageJ software. Protein levels were normalized to ribophorin I or α-tubulin.

immunofluorescence microscopy

Cells were plated in 6-well plates with acid-washed glass coverslips. After 24 h, cells were fixed with 4% paraformaldehyde (PFA) in DPBS for 30 min, washed five times with PBS, and permeabilized at room temperature with 0.1% Triton X-100 in DPBS for 15 min. Primary antibodies were used in 0.5% BSA in DPBS. Cells were incubated with blocking buffer (0.5% BSA in PBS) for 30 min at RT followed by 1 h incubation at RT with rabbit anti-FLAG antibody (1:500, Sigma-Aldrich, St. Louis, MO) and mouse anti-SEC31A antibody (1:500, BD Biosciences, Franklin Lakes, NJ) and then secondary antibodies such as Alexa Fluor 488 goat anti-rabbit IgG and Alexa Fluor 594 goat anti-mouse IgG (1:500, Molecular Probes, Invitrogen, Carlsbad, CA). Antibody incubations were followed by five PBS washes. Images were obtained using a confocal laser microscopy (Nikon C1, Nikon, Tokyo, Japan), and merges of images were processed using Nikon EZ-C1 viewer software.

Real-time quantitative PCR with reverse transcription

RNA was obtained from fibroblast cells using Trizol reagent (Invitrogen, Carlsbad, CA) according to the manufacturer's instructions. Complementary DNAs (cDNAs) were synthesized from total RNA using Superscript II First-strand Synthesis kit (Invitrogen, Carlsbad, CA) and quantified by real-time PCR using the IQ SYBR green supermix kit (Bio-Rad Laboratories, Hercules, CA) and the following primers: human *COL1A1*, 5′-GTGTTGTGCGATGACG-3′ and 5′-TCGGTGGGGTGACTCT-3′; human *GAPDH*, 5′-CTCCTCCACCTTTGACGC-3′ and 5′-CCACCACCCTGTTGCTGT-3′. Gene expression levels were normalized to *GAPDH* expression levels.

Statistical analysis

We performed Student's *t* test to assess the significance of differences between two groups of data. The results of multiple experiments were presented with mean±SD (SD). *p* values of less than 0.05 were considered statistically significant.

ACKNOWLEDGMENTS

We would like to thank the laboratories of Michael Rape and Randy Schekman for sharing valuable resources with us. Research reported in this publication was supported by the National Institute of General Medical Sciences of the National Institutes of Health under Award R01GM110373 and the National Institute of Arthritis and Musculoskeletal and Skin Diseases of the National Institutes of Health under Award R21AR075939.

REFERENCES

Akopian D, McGourty CA, Rape M (2022). Co-adaptor driven assembly of a CUL3 E3 ligase complex. Mol Cell 82, 585–597 e511.

Bachinger HP, Morris NP, Davis JM (1993). Thermal stability and folding of the collagen triple helix and the effects of mutations in osteogenesis imperfecta on the triple helix of type I collagen. Am J Med Genet 45, 152–162.

Bonfanti L, Mironov AA Jr, Martinez-Menarguez JA, Martella O, Fusella A, Baldassarre M, Buccione R, Geuze HJ, Mironov AA, Luini A (1998). Procollagen traverses the Golgi stack without leaving the lumen of cisternae: evidence for cisternal maturation. Cell 95, 993–1003.

Boyadjiev SA, Fromme JC, Ben J, Chong SS, Nauta C, Hur DJ, Zhang G, Hamamoto S, Schekman R, Ravazzola M, *et al*. (2006). Cranio-lenticulo-sutural dysplasia is caused by a SEC23A mutation leading to abnormal endoplasmic-reticulum-to-Golgi trafficking. Nat Genet 38, 1192–1197.

Canty EG, Kadler KE (2005). Procollagen trafficking, processing and fibrillogenesis. J Cell Sci 118, 1341–1353.
Fisher LW, Stubbs JT 3rd, Young MF (1995). Antisera and cDNA probes to human and certain animal model bone matrix noncollagenous proteins. Acta Orthop Scand Suppl 266, 61–65.
Furukawa M, He YJ, Borchers C, Xiong Y (2003). Targeting of protein ubiquitination by BTB-Cullin 3-Roc1 ubiquitin ligases. Nat Cell Biol 5, 1001–1007.
Garbes L, Kim K, Riess A, Hoyer-Kuhn H, Beleggia F, Bevot A, Kim MJ, Huh YH, Kweon HS, Savarirayan R, *et al.* (2015). Mutations in SEC24D, encoding a component of the COPII machinery, cause a syndromic form of osteogenesis imperfecta. Am J Hum Genet 96, 432–439.
Genschik P, Sumara I, Lechner E (2013). The emerging family of CULLIN3-RING ubiquitin ligases (CRL3s): cellular functions and disease implications. EMBO J 32, 2307–2320.
Gorrell L, Omari S, Makareeva E, Leikin S (2021). Noncanonical ER–Golgi trafficking and autophagy of endogenous procollagen in osteoblasts. Cell Mol Life Sci 78, 8283–8300.
Gorur A, Yuan L, Kenny SJ, Baba S, Xu K, Schekman R (2017). COPII-coated membranes function as transport carriers of intracellular procollagen I. J Cell Biol 216, 1745–1759.
He H, Peng Y, Fan S, Chen Y, Zheng X, Li C (2018). Cullin3/KCTD5 induces monoubiquitination of DeltaNp63alpha and impairs its activity. FEBS Lett 592, 2334–2340.
Jin L, Pahuja KB, Wickliffe KE, Gorur A, Baumgartel C, Schekman R, Rape M (2012). Ubiquitin-dependent regulation of COPII coat size and function. Nature 482, 495–500.
Kurz T, Pintard L, Willis JH, Hamill DR, Gonczy P, Peter M, Bowerman B (2002). Cytoskeletal regulation by the Nedd8 ubiquitin-like protein modification pathway. Science 295, 1294–1298.
Long KR, Yamamoto Y, Baker AL, Watkins SC, Coyne CB, Conway JF, Aridor M (2010). Sar1 assembly regulates membrane constriction and ER export. J Cell Biol 190, 115–128.
Lu CL, Kim J (2020). Consequences of mutations in the genes of the ER export machinery COPII in vertebrates. Cell Stress Chaperones 25, 199–209.
Lu CL, Ortmeier S, Brudvig J, Moretti T, Cain J, Boyadjiev SA, Weimer JM, Kim J (2022). Collagen has a unique SEC24 preference for efficient export from the endoplasmic reticulum. Traffic 23, 81–93.
McCaughey J, Stevenson NL, Cross S, Stephens DJ (2018). ER-to-Golgi trafficking of procollagen in the absence of large carriers. J Cell Biol 218, 929–948.
McCormick JA, Yang CL, Zhang C, Davidge B, Blankenstein KI, Terker AS, Yarbrough B, Meermeier NP, Park HJ, McCully B, *et al.* (2014). Hyperkalemic hypertension-associated cullin 3 promotes WNK signaling by degrading KLHL3. J Clin Invest 124, 4723–4736.
McGourty CA, Akopian D, Walsh C, Gorur A, Werner A, Schekman R, Bautista D, Rape M (2016). Regulation of the CUL3 ubiquitin ligase by a calcium-dependent co-adaptor. Cell 167, 525–538.e514.
Merlet J, Burger J, Gomes JE, Pintard L (2009). Regulation of cullin-RING E3 ubiquitin-ligases by neddylation and dimerization. Cell Mol Life Sci 66, 1924–1938.
Ohisa S, Inohaya K, Takano Y, Kudo A (2010). sec24d encoding a component of COPII is essential for vertebra formation, revealed by the analysis of the medaka mutant, vbi. Dev Biol 342, 85–95.
Omari S, Makareeva E, Roberts-Pilgrim A, Mirigian L, Jarnik M, Ott C, Lippincott-Schwartz J, Leikin S (2018). Noncanonical autophagy at ER exit sites regulates procollagen turnover. Proc Natl Acad Sci USA 115, E10099–E10108.
Petroski MD, Deshaies RJ (2005a). Function and regulation of cullin-RING ubiquitin ligases. Nat Rev Mol Cell Biol 6, 9–20.
Petroski MD, Deshaies RJ (2005b). Mechanism of lysine 48-linked ubiquitin-chain synthesis by the cullin-RING ubiquitin-ligase complex SCF-Cdc34. Cell 123, 1107–1120.
Pintard L, Willis JH, Willems A, Johnson JL, Srayko M, Kurz T, Glaser S, Mains PE, Tyers M, Bowerman B, *et al.* (2003). The BTB protein MEL-26 is a substrate-specific adaptor of the CUL-3 ubiquitin-ligase. Nature 425, 311–316.
Saha A, Deshaies RJ (2008). Multimodal activation of the ubiquitin ligase SCF by Nedd8 conjugation. Mol Cell 32, 21–31.
Sargeant J, Seiler DK, Costain T, Madreiter-Sokolowski CT, Gordon DE, Peden AA, Malli R, Graier WF, Hay JC (2021). ALG-2 and peflin regulate COPII targeting and secretion in response to calcium signaling. J Biol Chem 297, 101393.
Sarmah S, Barrallo-Gimeno A, Melville DB, Topczewski J, Solnica-Krezel L, Knapik EW (2010). Sec24D-dependent transport of extracellular matrix proteins is required for zebrafish skeletal morphogenesis. PLoS One 5, e10367.
Scott DC, Rhee DY, Duda DM, Kelsall IR, Olszewski JL, Paulo JA, de Jong A, Ovaa H, Alpi AF, Harper JW, *et al.* (2016). Two distinct types of E3 ligases work in unison to regulate substrate ubiquitylation. Cell 166, 1198–1214.e1124.
Soucy TA, Smith PG, Milhollen MA, Berger AJ, Gavin JM, Adhikari S, Brownell JE, Burke KE, Cardin DP, Critchley S, *et al.* (2009). An inhibitor of NEDD8-activating enzyme as a new approach to treat cancer. Nature 458, 732–736.
Stogios PJ, Downs GS, Jauhal JJ, Nandra SK, Prive GG (2005). Sequence and structural analysis of BTB domain proteins. Genome Biol 6, R82.
Townley AK, Feng Y, Schmidt K, Carter DA, Porter R, Verkade P, Stephens DJ (2008). Efficient coupling of Sec23-Sec24 to Sec13-Sec31 drives COPII-dependent collagen secretion and is essential for normal craniofacial development. J Cell Sci 121, 3025–3034.
Wang L, Lin M, Chu M, Liu Y, Ma J, He Y, Wang ZW (2020). SPOP promotes ubiquitination and degradation of LATS1 to enhance kidney cancer progression. EBioMedicine 56, 102795.
Xu L, Wei Y, Reboul J, Vaglio P, Shin TH, Vidal M, Elledge SJ, Harper JW (2003). BTB proteins are substrate-specific adaptors in an SCF-like modular ubiquitin ligase containing CUL-3. Nature 425, 316–321.
Zhu M, Tao J, Vasievich MP, Wei W, Zhu G, Khoriaty RN, Zhang B (2015). Neural tube opening and abnormal extraembryonic membrane development in SEC23A deficient mice. Sci Rep 5, 15471.